*Inorg. Chem.* **2005**, *44*, 5667–5676

# Synthesis, Structure, and Spectroscopic Properties of $Am(IO_3)_3$ and the Photoluminescence Behavior of $Cm(IO_3)_3$

**Richard E. Sykora,* Zerihun Assefa, and Richard G. Haire**

*Transuranium Research Laboratory, Chemical Sciences Division, Oak Ridge National Laboratory, Oak Ridge, Tennessee 37831*

**Thomas E. Albrecht-Schmitt**

*Department of Chemistry and Leach Nuclear Science Center, Auburn University, Auburn, Alabama 36849*

Received March 15, 2005

We have prepared $Am(IO_3)_3$ as a part of our continuing investigations into the chemistry of the 4f- and 5f-elements' iodates. Single crystals were obtained from the reaction of $Am^{3+}$ and $H_5IO_6$ under mild hydrothermal conditions. Crystallographic data on an eight-day-old crystal are (21 °C, Mo Kα, $\lambda = 0.71073$ Å): monoclinic, space group $P2_1/c$, $a = 7.2300(5)$ Å, $b = 8.5511(6)$ Å, $c = 13.5361(10)$ Å, $\beta = 100.035(1)°$, $V = 824.06(18)$, $Z = 4$. The structure consists of $Am^{3+}$ cations bound by iodate anions to form $[Am(IO_3)_8]$ units, where the local coordination environment around the americium centers is a distorted dodecahedron. There are three crystallographically unique iodate anions within the structure that bridge in both bidentate and tridentate fashions to form the overall three-dimensional structure. Repeated collection of X-ray diffraction data with time for a crystal of $^{243}Am(IO_3)_3$ revealed an anisotropic expansion of the unit cell, presumably from self-irradiation damage, to generate values of $a = 7.2159(7)$ Å, $b = 8.5847(8)$ Å, $c = 13.5715(13)$ Å, $\beta = 99.492(4)°$, $V = 829.18(23)$ after approximately five months. The $Am(IO_3)_3$ crystals have also been characterized by Raman spectroscopy and the spectral results compared to those for $Cm(IO_3)_3$. Three strong Raman bands were observed for both compounds and correspond to the I–O symmetric stretching of the three crystallographically distinct iodate anions. The Raman profile suggests a lack of interionic vibrational coupling of the I–O stretching, while intraionic coupling provides symmetric and asymmetric components that correspond to each iodate site. Photoluminescence data for both $Am(IO_3)_3$ and $Cm(IO_3)_3$ are reported here for the first time. Assignments for the electronic levels of the actinide cations were based on these photoluminescence measurements and indicate the presence of vibronic coupling between electronic transitions and $IO_3^-$ vibrational modes in both compounds.

## Introduction

The chemistry of transuranium iodates has been investigated previously in oxidation-state studies of plutonium in 1942[1] and tracer work with Am and Cm.[2] The separation of Bk from other transplutonium elements using iodate precipitation from homogeneous solution (PFHS) has also been reported.[3] The process is similar to the methods used to separate cerium from trivalent lanthanides,[4,5] where following oxidation of Ce(III), Ce(IV) iodate is precipitated from solution in the presence of excess iodate. Plutonium can be separated from alkali metals, lanthanides, uranium, and various fission products using similar processes.[6,7] In the case of $^{249}Bk$, iodate PFHS is attractive given that $^{249}Bk$ beta decays with a 320 day half life to $^{249}Cf$; therefore, iodate

* To whom correspondence should be addressed. E-mail: sykorare@ornl.gov. Phone: (865) 574-0846.

(1) Cunningham, B. B.; Werner, L. B. *J. Am. Chem. Soc.* **1949**, *71*, 1521.
(2) Thompson, S. G.; Morgan, L. O.; James, R. A.; Perlman, I. In *National Nuclear Energy Series, Manhattan Project Technical Section, Division 4*, Plutonium Project; Seaborg, G. T., Katz, J. J., Manning, W. M., Eds.; McGraw-Hill: New York, 1949; Vol. 14B, p 1339.
(3) Weaver, B. *Anal. Chem.* **1968**, *40*, 1894.
(4) Brinton, P. H. M.-P.; James, C. *J. Am. Chem. Soc.* **1919**, *41*, 1080.
(5) Willard, H. H.; T'Sai Yu, S. *Anal. Chem.* **1953**, *25*, 1754.
(6) Stoughton, R. W.; Duffield, R. B. U.S. Patent No. 2,856,261, 1958.
(7) Fries, B. A. U.S. Patent No. 2.926.067, 1960.

10.1021/ic050386k CCC: $30.25 
Published on Web 07/06/2005

PFHS offers a convenient approach to milk $^{249}$Cf(III) from solutions of $^{249}$Bk(IV).[3]

Although the chemistry of actinide iodates has been studied for decades,[1−3,6−11] only recently have detailed structural examinations been performed on them.[12−22] Initial investigations were with uranyl iodates[12−19] and extended to the heavier actinides with structural reports appearing on neptunyl,[17−20] plutonyl,[19−21] americium,[22] and curium[23] iodates. For uranium through plutonium, trans-dioxo units, $NpO_2^+$ or $AnO_2^{2+}$ (An = U, Np, Pu), are found in the structures of their iodates. Both $Pu(IO_3)_3$[9] and $Pu(IO_3)_4$ [1,24] have also been isolated, although their structures or even detailed compositions have not been reported. The structures of the americium(III) and curium(III) iodates are isostructural with lanthanide(III) iodates.[25−28] In addition to structural characterization with X-ray diffraction, spectroscopic characterization has also been reported for several of these actinide iodates.[12,19,23] The first Raman analysis of a trivalent, f-element iodate was reported for $Cm(IO_3)_3$,[23] where a significant shift of the I−O symmetric stretching frequency to higher wavenumbers was observed, as compared to previously reported transition-metal and actinide iodate systems.[19]

Transition-metal and lanthanide iodates have been more extensively studied, especially in the search for novel materials with interesting optical properties.[25−35] Nassau and co-workers prepared and characterized numerous structural families of 4f iodates[26,36,37] including the Type-I $Ln(IO_3)_3$ structure, which exists for the lanthanide(III) elements Ce−Lu, as well as for Cm and Y.[23,26,27] Douglas et al. recently reported single-crystal diffraction data for several of the members of this structural family;[25] the structures of additional lanthanide iodates have also been reported recently.[32,38,39]

The synthesis of transplutonium compounds, especially as single crystals, is complicated by the limited availability and short half lives of these elements. We recently reported the hydrothermal synthesis, single-crystal structure, Raman spectroscopy, and self-irradiation studies of $^{248}Cm(IO_3)_3$.[23] We are reporting here the synthesis, single-crystal structure, and the Raman and photoluminescence properties of $Am(IO_3)_3$ as well as the photoluminescence behavior of $Cm(IO_3)_3$. In addition, results of self-irradiation studies are presented for $^{243}Am(IO_3)_3$ and are compared with those for $^{248}Cm(IO_3)_3$.

## Experimental Section

**Materials and Methods.** The americium and curium isotopes used in these studies were made available by the U.S. Department of Energy. Triply distilled water was used in all reactions, and the $H_5IO_6$ (98%) was used as received from Alfa-Aesar. The aqueous $Am(NO_3)_3$ was prepared by dissolving Am metal in $HNO_3$, evaporating the resultant solution to dryness and then dissolving the solid product in $H_2O$. The isotopic purity of the americium was determined to be >99.9% $^{243}$Am by mass spectrometry analysis. Special training and experimental facilities are required in order to perform work with highly radioactive transuranium materials. Manipulations necessary to prepare $Am(IO_3)_3$ and $Cm(IO_3)_3$ were conducted in gloveboxes or hoods in accordance with established policies for handling radioactive materials at Oak Ridge National Laboratory. To prevent radioactive contamination, samples selected for analyses were doubly contained.

**Synthesis of $Am(IO_3)_3$.** The synthesis of $Am(IO_3)_3$ involved mixing $Am(NO_3)_3$ (10 $\mu$L, 0.14 M) and $H_5IO_6$ (43.2 $\mu$L, 0.10 M) in a 1 mL quartz reaction vessel. The reaction vessel was sealed, placed in a furnace, and then heated to 180 °C, where the reaction/crystallization occurred under autogenously generated pressure.[40] After 65 h, the furnace was cooled at 20 °C/h to 100 °C, turned off, and allowed to self-cool to room temperature. The product consisted of yellow, irregular crystals of $Am(IO_3)_3$ as well as trace quantities of an unidentified pink solid in a colorless mother liquor.


(8) Seaborg, G. T.; Wahl, A. C. *J. Am. Chem. Soc.* **1948**, *70*, 1128.
(9) Anderson, H. H. In *National Nuclear Energy*, Manhattan Project Technical Section, Division 4, Plutonium Project; Seaborg, G. T., Katz, J. J., Manning, W. M., Eds.; McGraw-Hill: New York, 1949; Vol. 14B, p 825.
(10) (a) Weigel, F.; Engelhardt, L. *J. Less-Common Met.* **1983**, *91*, 339. (b) Hall, D. *J. Inorg. Nucl. Chem.* **1958**, *6*, 3.
(11) Meyer, R. J.; Speter, M. *Chem.-Ztg.* **1910**, *34*, 306.
(12) Bean, A. C.; Peper, S. M.; Albrecht-Schmitt, T. E. *Chem. Mater.* **2001**, *13*, 1266.
(13) Bean, A. C.; Ruf, M.; Albrecht-Schmitt, T. E. *Inorg. Chem.* **2001**, *40*, 3959.
(14) Bean, A. C.; Albrecht-Schmitt, T. E. *J. Solid State Chem.* **2001**, *161*, 416.
(15) Shvareva, T. Y.; Almond, P. M.; Albrecht-Schmitt, T. E. *J. Solid State Chem.* **2005**, *178*, 499.
(16) Sykora, R. E.; McDaniel, S. M.; Wells, D. M.; Albrecht-Schmitt, T. E. *Inorg. Chem.* **2002**, *41*, 5126.
(17) Sykora, R. E.; Bean, A. C.; Scott, B. L.; Runde, W.; Albrecht-Schmitt, T. E. *J. Solid State Chem.* **2004**, *177*, 725.
(18) Albrecht-Schmitt, T. E.; Almond, P. M.; Sykora, R. E. *Inorg. Chem.* **2003**, *42*, 3788.
(19) Bean, A. C.; Scott, B. L.; Albrecht-Schmitt, T. E.; Runde, W. *Inorg. Chem.* **2003**, *42*, 5632.
(20) Bean, A. C.; Scott, B. L.; Albrecht-Schmitt, T. E.; Runde, W. *J. Solid State Chem.* **2004**, *177*, 1346.
(21) Runde, W.; Bean, A. C.; Albrecht-Schmitt, T. E.; Scott, B. L. *Chem. Commun.* **2003**, 478.
(22) Runde, W.; Bean, A. C.; Scott, B. L. *Chem. Commun.* **2003**, 1848.
(23) Sykora, R. E.; Assefa, Z.; Haire, R. G.; Albrecht-Schmitt, T. E. *J. Solid State Chem.* **2004**, *177*, 4413.
(24) Sklyarenko, I. S.; Chubukova, T. M. *Zh. Anal. Khim.* **1963**, *18*, 492.
(25) Douglas, P.; Hector, A. L.; Levason, W.; Light, M. E.; Matthews, M. L.; Webster, M. *Z. Anorg. Allg. Chem.* **2004**, *630*, 479.
(26) Abrahams, S. C.; Bernstein, J. L.; Nassau, K. *J. Solid State Chem.* **1976**, *16*, 173.
(27) Liminga, R.; Abrahams, S. C.; Bernstein, J. L. *J. Chem. Phys.* **1977**, *67*, 1015.
(28) Sykora, R. E.; Albrecht-Schmitt, T. E., unpublished results.
(29) Sykora, R. E.; Ok, K. M.; Halasyamani, P. S.; Wells, D. M.; Albrecht-Schmitt, T. E. *Chem. Mater.* **2002**, *14*, 2741.
(30) Sykora, R. E.; Ok, K. M.; Halasyamani, P. S.; Albrecht-Schmitt, T. E. *J. Am. Chem. Soc.* **2002**, *124*, 1951.
(31) Bentria, B.; Benbertal, D.; Bagieu-Beucher, M.; Mosset, A. *Z. Anorg. Allg. Chem.* **2004**, *630*, 781.
(32) Hector, A. L.; Henderson, S. J.; Levason, W.; Webster, M. *Z. Anorg. Allg. Chem.* **2002**, *628*, 198.
(33) Abrahams, S. C.; Sherwood, R. C.; Bernstein, J. L.; Nassau, K. *J. Solid State Chem.* **1973**, *7*, 205.
(34) Abrahams, S. C.; Sherwood, R. C.; Bernstein, J. L.; Nassau, K. *J. Solid State Chem.* **1973**, *8*, 274.
(35) Abrahams, S. C.; Bernstein, J. L. *Solid State Commun.* **1978**, *27*, 973.
(36) Nassau, K.; Shiever, J. W.; Prescott, B. E. *J. Solid State Chem.* **1975**, *14*, 122.
(37) Nassau, K.; Shiever, J. W.; Prescott, B. E.; Cooper, A. S. *J. Solid State Chem.* **1974**, *11*, 314.
(38) Hector, A. L.; Levason, W.; Webster, M. *Inorg. Chim. Acta* **2000**, *298*, 43.
(39) Sykora, R. E.; Deakin, L.; Mar, A.; Skanthakumar, S.; Soderholm, L.; Albrecht-Schmitt, T. E. *Chem. Mater.* **2004**, *16*, 1343.

(40) The pressure was not measured but was calculated to be ~2 atm at 180 °C using the van der Waals' equation of state. This calculation was made under the assumption that the only components of the reaction vessel were 1 atm of air (at room temperature), water, and oxygen (generated during the reduction of periodate).

**Table 1.** Crystallographic Data[a] for $Am(IO_3)_3$

| | |
|---|---|
| chemical formula | $Am(IO_3)_3$ |
| formula mass | 767.76 |
| space group | $P2_1/c$ (No. 14) |
| $a$ (Å) | 7.2300(5) |
| $b$ (Å) | 8.5511(6) |
| $c$ (Å) | 13.5361(10) |
| $\beta$ (deg) | 100.035(1) |
| $V$ (Å$^3$) | 824.06(18) |
| Z | 4 |
| $T$ (°C) | 21 |
| $\lambda$ (Å) | 0.71073 |
| $D_{calcd}$ (g cm$^{-3}$) | 6.188 |
| $\mu$(Mo K$\alpha$) (cm$^{-1}$) | 205.73 |
| $R(F_o)$ for $F_o^2 > 2\sigma(F_o^2)$[b] | 0.0292 |
| $R_w(F_o^2)$[c] | 0.0763 |

[a] Crystals of $Am(IO_3)_3$ are affected by self-irradiation. Values provided are for an eight-day-old crystal. [b] $R(F_o) = \sum||F_o| - |F_c||/\sum|F_o|$. [c] $R_w(F_o^2) = [\sum[w(F_o^2 - F_c^2)^2]/\sum wF_o^4]^{1/2}$.

**Single-Crystal X-ray Diffraction.** A selected crystal of $Am(IO_3)_3$, with dimensions of 0.259 mm × 0.212 mm × 0.162 mm, was sealed in a capillary, placed inside of a polyethylene tube for secondary containment, and aligned on a Bruker SMART APEX CCD X-ray diffractometer with a digital camera. Intensity measurements were performed using graphite-monochromated, MoK$\alpha$ radiation from a sealed X-ray tube with a monocapillary collimator. The intensities of reflections of a sphere were collected by a combination of three sets of exposure frames. Each set had a different $\varphi$ angle for the crystal, and each exposure covered a range of 0.3° in $\omega$. A total of 1800 frames were collected with an exposure time per frame of 30 s.

The determination of integrated intensities and a global cell refinement were performed with the Bruker SAINT (v 6.02) software package using a narrow-frame, integration algorithm. A semiempirical absorption correction was applied using SADABS.[41] The program suite SHELXTL (v 5.1) was used for space group determination (XPREP), direct methods structure solution (XS), and least-squares refinement (XL).[42] The scattering factor, real and imaginary dispersion terms, and the linear absorption coefficient for americium[43] were manually added into the SHELXTL instruction files. The final refinements included anisotropic displacement parameters for all atoms and a secondary extinction parameter. Some crystallographic details are listed in Table 1; additional details can be found in the Supporting Information.

**Raman Spectroscopy.** Raman spectra were obtained on room-temperature samples using an argon-ion laser (Coherent, model 306) and a double-meter spectrometer (Jobin-Yvon Ramanor model HG.2S). The resolution of the monochromator is 0.5 cm$^{-1}$. The monochromator is interfaced with a personal computer; scanning and data collections are controlled by LabSpec (version 3.04) software. Signal detection was with a water-cooled photomultiplier tube (Hamamatsu R636).

**Photoluminescence Studies.** The 457-nm argon laser line was used for the excitation of $Cm(IO_3)_3$, and the 514.5-nm line was used for the excitation of $Am(IO_3)_3$. The luminescence spectra were collected on samples at room temperature using an Instrument SA optical system consisting of a monochromator (model 1000M) attached to charge-coupled device, PMT, and IR detectors. Additional higher resolution spectra were collected using a HG.2S monochromator at a scanning step of 6 cm$^{-1}$. Data analyses were performed with Grams/32 software (Galactic, version 5.1).

## Results and Discussion

**Synthesis.** Immediately upon mixing of the $Am^{3+}$ and $H_5IO_6$ solutions an unidentified precipitate was formed. It is probable that this precipitate was an americium periodate complex, as $Y(H_2O)_3\{IO_4(OH)_2\}$[38] has been reported to form under similar reaction conditions. Relatively large yellow crystals of $Am(IO_3)_3$ with an irregular habit were formed by the subsequent heating of the reaction solution and the initial precipitate. The reduction of the periodate to iodate under similar reaction conditions has been previously reported.[23,25] A minor amount (<1% of product) of an unidentified pink powder was observed as a byproduct of this reaction, but it was not practical to analyze this material given it's small quantity. The pink color is indicative of Am(III) and could represent the isolation of an additional americium iodate product. Further investigations would be necessary to determine the nature of this material.

**Description of the Crystal Structure.** $Am(IO_3)_3$ was determined to be isostructural with Type I $Gd(IO_3)_3$. This structure has also been reported for all of the lanthanides,[26] except Pm, as well as for Y[26] and Cm.[23] Detailed structural data, including atomic positions, have only been reported for the Type I Gd,[27] Tb,[25] and Cm iodates.[23]

In the structure, the americium atom is coordinated by eight oxygen atoms forming a distorted dodecahedral arrangement, as found for the other Type I f-element iodates. The method given by Lippard and Russ[44] was used to verify this assignment, since the determination between distorted dodecahedral and distorted square antiprismatic coordination is not always straightforward. Each $AmO_8$ polyhedron is formed by the monodentate coordination of eight iodate anions: two $I(1)O_3^-$, three $I(2)O_3^-$, and three $I(3)O_3^-$ anions, as shown in Figure 1.

The Am(1) sites are linked by both ($I(1)O_3^-$) and ($I(3)O_3^-$) iodate ligands into layers present in the crystallographic (*bc*) plane (Figure 2). These layers are further connected by ($I(2)O_3^-$) anions into a three-dimensional network. A ball-and-stick representation of the $Am(IO_3)_3$ structure, as viewed down the crystallographic *b* axis, is shown in Figure 3.

The Am−O bond lengths for the americium polyhedra range from 2.330(5) to 2.584(5) Å for $Am(IO_3)_3$. These distances are within the ranges expected, as calculated from published radii,[45] and as reported previously.[22,46] These values result in a bond valence sum of 3.29 for americium.[47] The iodate anions have bond lengths from 1.784(5) to 1.818(6) Å, consistent with values found in other lanthanide and actinide iodates.[16,23,27] In addition to these three short I−O distances, there are additional I···O contacts for each iodine

(41) SADABS. Program for absorption correction using SMART CCD based on the method of Blessing: Blessing, R. H. *Acta Crystallogr.* **1995**, *A51*, 33.
(42) Sheldrick, G. M. *SHELTXL PC, Version 5.0, An integrated system for solving, refining, and displaying crystal structures from diffraction data*; Siemens Analytical X-ray Instruments, Inc.: Madison, WI, 1994.
(43) Wilson, A. J. C. *International Tables for Crystallography, Vol. C, Mathematical, Physical and Chemical Tables*; Kluwer Academic Publishers: Boston, 1992.
(44) Lippard, S. J.; Russ, B. J. *Inorg. Chem.* **1968**, *7*, 1686.
(45) Shannon, R. D. *Acta Crystallogr.* **1976**, *A32*, 751.
(46) Burns, J. H.; Baldwin, W. H. *Inorg. Chem.* **1977**, *16*, 289.
(47) Brese, N. E.; O'Keeffe, M. *Acta Crystallogr.* **1991**, *B47*, 192.

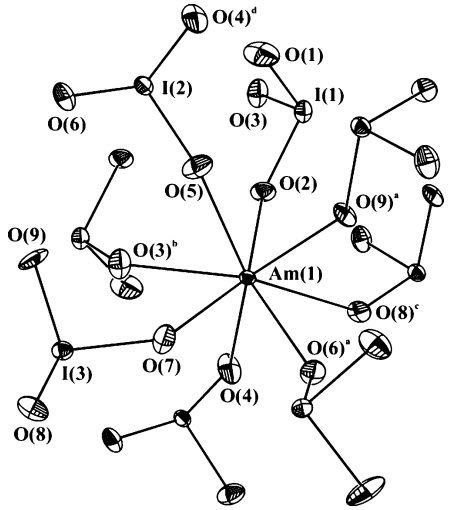


**Figure 1.** An illustration of the distorted dodecahedral environment around the $Am^{3+}$ centers in $Am(IO_3)_3$. 50% displacement ellipsoids are shown.

**Table 2.** Selected Bond Distances (Å) and Angles (deg) for $Am(IO_3)_3$[e]

| Bond Distances (Å) | | | |
|---|---|---|---|
| Am(1)−O(2) | 2.364(5) | I(1)−O(1) | 1.791(6) |
| Am(1)−O(3)[b] | 2.520(5) | I(1)−O(2) | 1.805(5) |
| Am(1)−O(4) | 2.330(5) | I(1)−O(3) | 1.805(5) |
| Am(1)−O(5) | 2.489(5) | I(2)−O(4)[d] | 1.784(5) |
| Am(1)−O(6)[a] | 2.422(5) | I(2)−O(5) | 1.807(5) |
| Am(1)−O(7) | 2.476(6) | I(2)−O(6) | 1.800(5) |
| Am(1)−O(8)[c] | 2.584(5) | I(3)−O(7) | 1.818(6) |
| Am(1)−O(9)[a] | 2.393(5) | I(3)−O(8) | 1.794(5) |
| | | I(3)−O(9) | 1.789(6) |
| **Angles (deg)** | | | |
| O(1)−I(1)−O(2) | 101.0(3) | O(5)−I(2)−O(6) | 99.1(3) |
| O(1)−I(1)−O(3) | 100.8(3) | O(7)−I(3)−O(8) | 103.0(3) |
| O(2)−I(1)−O(3) | 97.8(3) | O(7)−I(3)−O(9) | 97.3(3) |
| O(4)−I(2)−O(5) | 96.7(3) | O(8)−I(3)−O(9) | 96.9(3) |
| O(4)−I(2)−O(6) | 96.6(3) | | |

[a] $1-x, {}^1/_2+y, {}^1/_2-z$. [b] $1-x, -y, -z$. [c] $x, {}^1/_2-y, z-{}^1/_2$. [d] $x-1, y, z$. [e] Crystals of $Am(IO_3)_3$ are affected by self-irradiation. Values are for the eight-day-old crystal.

atom from the oxygen atoms of neighboring iodate anions. The I(1) exhibits 7-fold coordination forming a polyhedron best described as a monocapped trigonal prism, as a result of three short I−O bonds with distances from 1.791(6) to 1.805(5) Å, two intermediate I−O distances of 3.056(6) and 3.069(6) Å, and two long I−O contacts of 3.306(6) and 3.327(6) Å. The iodate anions containing I(2) and I(3) have three longer contacts from 2.743(6) to 2.998(6) Å and 2.816(6) to 3.093(6) Å, respectively, in addition to the three oxygen atoms found in the inner sphere of each iodine atom. The six-coordinate polyhedra for I(2) and I(3) are highly distorted. Similar bonding arrangements for I(V) are found in previously reported iodates.[23,27,48] The calculated bond valence sums, using only inner sphere oxygen atoms, for the iodine atoms in $Am(IO_3)_3$ are 5.15, 5.15, and 5.19, consistent with I(V).[47] A detailed list of bond lengths and angles for $Am(IO_3)_3$ is given in Table 2.

**Effects of Self-Irradiation on $Am(IO_3)_3$ and $Cm(IO_3)_3$.** The effects of radioactive decay on materials can be very complex, especially in the special case where the decaying atoms make up the matrix itself (self-irradiation). The electromagnetic radiation, particles (alpha, beta, neutrons), as well as the recoiling nuclei or fission fragments all initiate reactions in materials; the effects on crystal matrixes by different decay processes have been studied over the years.[49−51] There is also thermal energy generated accompanying the decay, and collisions with atoms of the lattice may also be significant. The accompanying heat is higher in $^{243}$Am than $^{248}$Cm; the specific heat of decay for $^{243}$Am is 6.28 mW/g,[52] and the value for $^{248}$Cm is 0.117 mW/g.[52] Given that the samples are on the order of micrograms, their thermal outputs are not significant.

As part of our studies of $Am(IO_3)_3$ in this work and former work on $Cm(IO_3)_3$,[23] we followed the stability of these iodate materials with regard to self-irradiation with time. It is useful to compare here the behavior of these two materials with time and their radiation processes. The work on $Am(IO_3)_3$ employed the $^{243}$Am isotope, an alpha emitter having a half life of $7.38 \times 10^3$ years. In contrast, the related study of $Cm(IO_3)_3$ was performed with a mixture of $^{246}$Cm (3%) and $^{248}$Cm (97%) isotopes, both of which have alpha decay paths but also emit neutrons and fragments from spontaneous fission (see Table 3). Thus, the $Am(IO_3)_3$ crystals were subjected to both alpha particles (kinetic energies up to 5.266 MeV)[52] plus the recoiling nucleus. In the case of $Cm(IO_3)_3$, it encountered both of the above (with up to 5.376 MeV alpha particles)[52] but also neutrons ($4.2 \times 10^7$ neutrons $s^{-1}$ $g^{-1}$)[53] and fission fragments from spontaneous fission processes.

On the basis of other work and information,[54] we did not expect oxidation or reduction of the actinide metal ions in these compounds. Rather, we assumed that the vulnerable part of the crystals may be the iodate anions; lattice expansion and the destruction of the materials' crystallinity presumably would be a result of iodine reduction or dislocations in the lattice.

With the single crystals of $Am(IO_3)_3$, the color of the crystals was observed to change from yellow to orange and then to red over the course of several months, but as in the case of $Cm(IO_3)_3$[23] the sample continued to diffract well. Analyses of the diffraction data showed a gradual loss of crystallinity with time, resulting in poorer refinements and larger atomic displacement parameters. The cell parameters showed anisotropic effects due to the self-irradiation, as seen in Table 4, with an overall increase in the cell volume of ∼0.6%. An initial increase in the three axes and a slight decrease in the $\beta$ angle was observed, while with additional

(48) Cooper, M. A.; Hawthorne, F. C.; Roberts, A. C.; Grice, J. D.; Stirling, J. A. R.; Moffatt, E. A. *Am. Mineral.* **1998**, *83*, 390.

(49) Fuger, J.; Matzke, Hj. In *Handbook on the Physics and Chemistry of the Actinides*; Freeman, A. J., Keller, C., Eds.; North-Holland, 1991; Vol. 6, p 641−84 and references therein.

(50) Alenchikova, F.; Zaitseva, L. L.; Lipis, L. V.; Fomin, V. V. *Russ. J. Inorg. Chem.* **1959**, *4*, 961.

(51) Young, J. P.; Haire, R. G.; Peterson, J. R.; Ensor, D. D.; Fellows, R. L. *Inorg. Chem.* **1980**, *19*, 2209.

(52) U.S. Department of Energy, Office of Environmental Management, http://web.em.doe.gov/idb97/tabb1.html.

(53) Shleien, B. *The Health Physics and Radiological Health Handbook*; Scinta, Inc.: Silver Spring, MD, 1992.

(54) Haire, R. G.; Stump, N. A. In *Materials Research Society Symposium Proceedings*; Gray, W. J., Triay, I. R., Eds.; Materials Research Society: Pittsburgh, PA, 1997; Vol. 465, p 39.

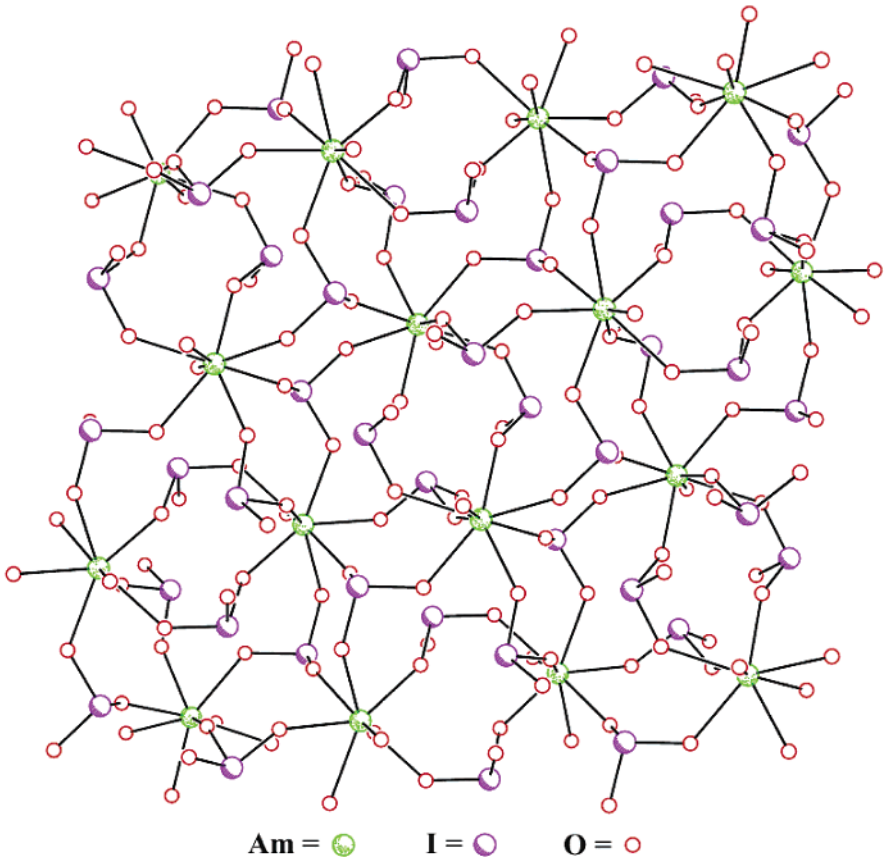


**Figure 2.** Americium iodate layers found in the crystallographic (*bc*) plane of $Am(IO_3)_3$. Both bidentate and tridentate iodate anions are found bridging the $AmO_8$ polyhedra in these layers.

**Table 3.** Radioactive Properties for Select Am and Cm Isotopes

| isotope | $^{243}$Am | $^{248}$Cm | $^{246}$Cm | Cm mixture[a] |
|---|---|---|---|---|
| half life[b] (years) | $7.38 \times 10^3$ | $3.40 \times 10^5$ | $4.73 \times 10^3$ | |
| specific activity[b] (Ci $g^{-1}$) | 0.1993 | $4.251 \times 10^{-3}$ | 0.3072 | |
| alpha rate[c] ($\alpha$ $s^{-1}$ $g^{-1}$) | $7.38 \times 10^9$ | $1.44 \times 10^8$ | $1.14 \times 10^{10}$ | $4.82 \times 10^8$ |
| fission fraction[d] (%) | | 8.39 | 0.0263 | |
| neutrons per fission[d] | | 3.157 | 2.95 | |
| neutron rate[d] (n $s^{-1}$ $g^{-1}$) | | $4.2 \times 10^7$ | $8.8 \times 10^6$ | $4.1 \times 10^7$ |

[a] 3% $^{246}$Cm, 97% $^{248}$Cm. Curium is typically isolated from californium parents in this ratio. [b] Values taken from ref 52. [c] Calculated based on half life from ref 52 and fission fraction in ref 53. [d] Values taken from ref 53.

**Table 4.** Radiation-Induced Lattice Expansion of $^{243}Am(IO_3)_3$

| sample age[a] | *a* (Å) | *b* (Å) | *c* (Å) | $\beta$ (deg) | *V* (Å$^3$) | % volume expansion |
|---|---|---|---|---|---|---|
| 8 days | 7.2300(5) | 8.5511(6) | 13.5361(10) | 100.035(1) | 824.06(18) | |
| 23 days | 7.2321(6) | 8.5617(7) | 13.5475(11) | 99.949(1) | 826.23(12) | 0.26 |
| 59 days | 7.2254(6) | 8.5690(7) | 13.5519(11) | 99.763(1) | 826.91(20) | 0.35 |
| 143 days | 7.2159(7) | 8.5847(8) | 13.5715(13) | 99.492(4) | 829.18(23) | 0.62 |

[a] The first data collection was made after 8 days; some effects had likely occurred before this time. (Experimental circumstances precluded the immediate examination of the crystals.)

aging, the *a* axis as well as $\beta$ decreased, while the *b* and *c* axes remained larger than those in the original material.

The anisotropic swelling in the crystallographic axes of $Am(IO_3)_3$ reflects changes in the iodate layers found in the crystallographic (*bc*) plane (Figure 2) due to a swelling parallel to these layers. The observed decrease in *a* is a result of the decreased interlayer spacing, while the decreased angle $\beta$ is a result of the shifting of the iodate layers relative to one another. The continued expansion in the americium iodate layers along *b* and *c* eventually gives rise to a more efficient packing arrangement and allows the layers to shift and move closer together resulting in the decrease of *a*. In $Cm(IO_3)_3$,[23] lattice swelling was observed along all three crystallographic axes followed by a general loss of crystallinity. In general, both materials showed an overall cell expansion with self-irradiation, although the $Cm(IO_3)_3$ crystals changed more rapidly and underwent physical breakup more readily.

The effect of cell expansion in $^{243}Am(IO_3)_3$ is assumed to be due to alpha particles together with damage from the recoiling nuclei. With $Cm(IO_3)_3$,[23] the specific alpha activity was lower than for the $^{243}Am(IO_3)_3$ crystals (Table 3), but

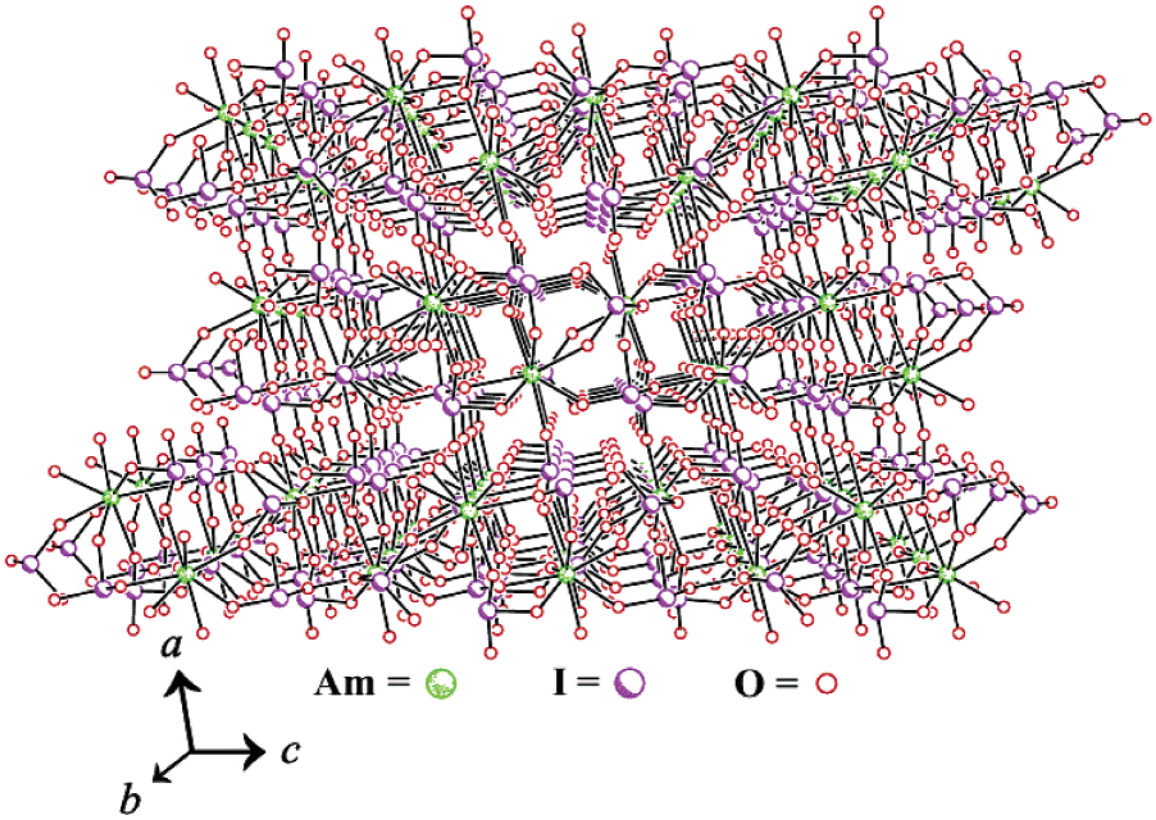


**Figure 3.** The three-dimensional network structure of $Am(IO_3)_3$ as viewed down the *b* axis.

neutrons and fission fragments also played a role in the changes observed with time. The bottom line is that the $Am(IO_3)_3$ crystals retained their crystallinity for a longer period than the $Cm(IO_3)_3$ crystals.

We propose that the alpha radiation and recoiling nuclei caused dislocations of the lattice components, especially in the iodate anions, and possibly led to some chemical reduction of these anions. It seems likely that some damage due to alpha decay occurred in the $Cm(IO_3)_3$ crystals but that damage from the fission fragments and neutrons was more important. It is speculated that, given a more similar mass of each, the neutrons could efficiently transfer kinetic energy to the oxygen atoms of the iodate anions by direct collisions. Dislocation of the oxygen atoms from the anions together with ionization radiation may have generated some molecular iodine, which would give rise to the color changes observed. In both actinide materials, it is believed that potential changes with the iodate anions may be the key aspect of the destruction process observed.

**Raman Spectroscopy.** Raman spectra of polycrystalline iodate salts of monovalent and divalent alkaline and alkaline earth metal ions have been reported previously.[19,55−60] With iodate salts of mono- and divalent cations, the comparison criteria for Raman band assignments include relative intensities, energy positions, and I−O bond strengths.[55−60] In pyramidal iodate ions with $C_{3v}$ symmetry, the three I−O stretching motions couple to the symmetric $IO_3^-$ stretching mode ($\nu_1$) and the degenerate asymmetric stretch, $\nu_3$. Similar couplings also occur for the pyramidal $ClO_3^-$ and $BrO_3^-$ ions in $C_{3v}$ symmetry.[59] In contrast, systems with large distortions from the $C_{3v}$ symmetry are characterized by a lack of intraionic coupling of the three X−O vibrations, and the degeneracy of the $\nu_3$ mode is removed in such systems.

In a recent paper we have reported the crystal structure and Raman spectrum of isostructural $Cm(IO_3)_3$;[23] $Am(IO_3)_3$ has nearly identical structural parameters and possesses a similar coordination environment around the actinide ion. The presence of three distinct iodate ions is a characteristic feature of these compounds. As all the atoms in the unit cell occupy 4*e* Wyckoff sites (general positions containing $C_1$ site symmetry), the three crystallographically distinct iodate ions have lower site symmetry ($C_1$) than the pyramidal $C_{3v}$ (3*m*) symmetry expected for an isolated $IO_3^-$ ion.

Collection of the Raman spectrum for $Am(IO_3)_3$ was limited to the $IO_3^-$ stretching and bending regions, 600−950 and 100−500 $cm^{-1}$, respectively. The Raman spectrum of the $Am(IO_3)_3$ crystal over the $\nu_{I-O}$ stretching region is compared to that for $Cm(IO_3)_3$ in Figure 4. For $Am(IO_3)_3$, the I−O stretching region consists of three strong bands at 760, 801, and 842 $cm^{-1}$ and weaker bands at 719 and 738 $cm^{-1}$. As with the curium iodate spectrum,[23] a unique strong band at a relatively high frequency is also observed. The

(55) Pracht, G.; Lange, N.; Lutz, H. D. *Thermochim. Acta* **1997**, *293*, 13.
(56) Lutz, H. D.; Alici, E.; Kellersohn, Th. *J. Raman Spectrosc.* **1990**, *21*, 387.
(57) During, J. R.; Bonner, O. D.; Breazeale, W. H. *J. Phys. Chem.* **1965**, *69*, 3886.
(58) Schellenschlager, V.; Pracht, G.; Lutz, H. D. *J. Raman Spectrosc.* **2001**, *32*, 373.
(59) Lutz, H. D.; Suchanek, E. *Spectrochim. Acta* **2000**, *A56*, 2707.
(60) Pracht, G.; Nagel, R.; Suchanek, E.; Lange, N.; Lutz, H. D. Z. *Anorg. Allg. Chem.* **1998**, *624*, 1355.

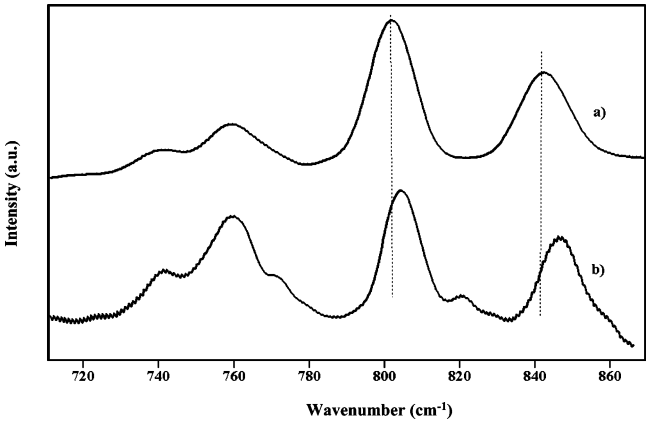


**Figure 4.** Comparison of Raman spectrum of (a) $Am(IO_3)_3$ and (b) $Cm(IO_3)_3$ in the I−O stretching region. The vertical dot lines are drawn to guide the eye on the Raman shift.

appearance of a strong stretching band at >840 $cm^{-1}$ for both compounds is intriguing, as the average I−O frequency reported for iodate salts of mono- and divalent cations is ∼770 $cm^{-1}$,[55,61] and the strongest symmetric stretching band for actinyl iodates is located at ∼785 $cm^{-1}$.[19]

This high-energy band appears to be uniquely associated with trivalent cation salts, as both $Cm(IO_3)_3$ and $Am(IO_3)_3$ display it at >840 $cm^{-1}$. We have also undertaken Raman measurements on neodymium iodate crystals and have found a high-energy symmetric stretching band at 852 $cm^{-1}$, indicating that f-element trivalent cations induce significant shifts to the I−O stretching mode. Close comparison of the $Am(IO_3)_3$ and $Cm(IO_3)_3$ spectra indicate that the highest-stretching band slightly red shifts to 842 $cm^{-1}$ for $Am(IO_3)_3$ as compared to 846 $cm^{-1}$ for $Cm(IO_3)_3$. The I−O band at 801 $cm^{-1}$ is also red shifted slightly as compared to the same band of $Cm(IO_3)_3$ found at 804 $cm^{-1}$.

Inspection of the crystal structure reveals that the shortest Am−O distance (2.330 Å) corresponds to an oxygen atom, O(4), from $I(2)O_3^-$. This distance is significantly shorter (>0.25 Å) than the longest Am−O distance (2.584 Å) associated with $I(3)O_3^-$. On the average, the Am−O distances to $I(2)O_3^-$ are shorter by ∼0.03 and 0.07 Å as compared to the Am−O distances formed with $I(1)O_3^-$ and $I(3)O_3^-$, respectively. Similar differences in Cm−O distances were noted in $Cm(IO_3)_3$.[23] We propose that the trivalent cation affects the I(2) site by withdrawing more electron density from it than the other two sites, resulting in the shift of the $\nu_{I-O}$ vibrational band for $I(2)O_3^-$ to a higher wavenumber, relative to the other iodates.

**Photoluminescence Studies. $Am(IO_3)_3$.** The photoluminescence spectrum of crystalline $Am(IO_3)_3$ is shown in Figure 5. The 514.5-nm laser line, which is nearly in resonance with the $^5L_{6'}$ level, was used in these excitations. The prime on the J quantum number indicates that the Russell−Saunders coupling scheme is not strictly valid for the actinides[62] because of the comparable strength of the spin−orbit and the electron−electron interactions. The L−S component that

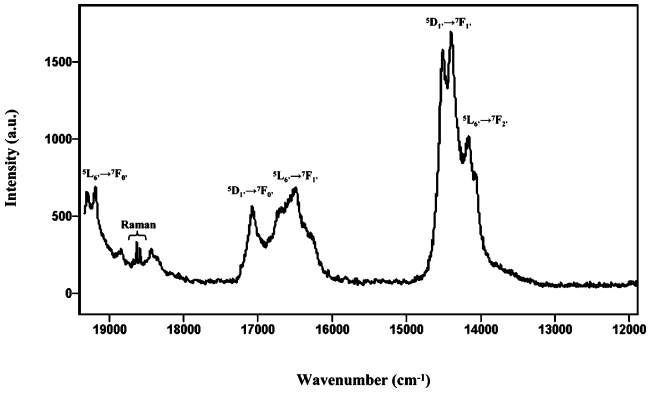


**Figure 5.** Emission spectrum of $Am(IO_3)_3$ collected using the 514.5-nm line of an argon laser. The peaks assigned to vibronic coupling are not labeled.

makes the dominant contribution to the wave function is used in labeling the J values.[63,64] The $Am(IO_3)_3$ emissions consist of a series of three groups of bands that originate from two different excited states. The first of these features is observed as a doublet with peaks located at 19 300 and 19 200 $cm^{-1}$ and correspond to the $^5L_{6'} \rightarrow {}^7F_{0'}$ transition.[65] The ground state of $Am^{3+}$ (isoelectronic with that of $Eu^{3+}$) has a configuration of six f electrons in a $J = 0$ state. Hence the $^7F_{0'}$ state is not expected to show splitting, and the observance of a doublet with a 100 $cm^{-1}$ separation is indicative of thermal population of higher Stark components of the emitting-state manifold.[66]

The sharper bands at 18 670, 18 640, and 18 600 $cm^{-1}$ are actually Raman bands since they are located at Stokes shifts of ∼765, ∼800, and ∼840 $cm^{-1}$ from the excitation wavelength.[62,65,67,68] The bands match very well with the Raman bands shown in Figure 4 both in terms of relative intensities and energy positions. In addition, two broader bands are observed at 18 850 and 18 430 $cm^{-1}$. The assignments of these bands have not been straightforward since no purely electronic f−f transition for $Am^{3+}$ is expected in this region. We will discuss the nature of these bands below.

The second group of the emission profile consists of a combination of sharp bands overlaying a broader feature in the 17 500−16 000 $cm^{-1}$ region. The sharp band that centers at 17 080 $cm^{-1}$ corresponds to the $^5D_{1'} \rightarrow {}^7F_{0'}$ transition, while the band at 16 490 $cm^{-1}$ corresponds to emissions originating from the higher $^5L_{6'} \rightarrow {}^7F_{1'}$ transitions.[62,65] This band is broader than observed in other americium systems;[69] the breadth of this band will be discussed in more detail below. The most intense band appears as a doublet with peaks at 14 520 and 14 410 $cm^{-1}$. The low-energy side of the band exhibits shoulders at 14 165 and 14 065 $cm^{-1}$. The portion of the emission spectrum covering the 15 000−

(61) Kellersohn, Th.; Alici, E.; Eber, D.; Lutz, H. D. *Z. Kristallogr.* **1993**, *203*, 225.
(62) Valenzuela, R. W.; Brundage, R. T. *J. Chem. Phys.* **1990**, *93*, 8469.
(63) Carnall, W. T.; Rajnak, K. *J. Chem. Phys.* **1975**, *63*, 3510.
(64) Carnall, W. T.; Fields, P. R. *Adv. Chem. Ser.* **1967**, *71*, 86.
(65) Beitz, J. V.; Brundage, R. T. *J. Alloys Compd.* **1992**, *181*, 49.
(66) Williams, M.; Brundage, R. T. *Phys. Rev.* **1992**, *B45*, 4561.
(67) Shiloh, M.; Givon, M.; Marcus, Y. *J. Inorg. Nucl. Chem.* **1969**, *31*, 1807.
(68) Henrie, D. E.; Fellows, R. L.; Choppin, G. R. *Coord. Chem. Rev.* **1976**, *18*, 199.
(69) Hubert, S.; Thouvenot, P. *J. Alloys Comp.* **1992**, *180*, 193.

13 000-$cm^{-1}$ region is known to represent transitions originating from two different excited states due to the overlap of the $^5L_{6'} \rightarrow {}^7F_{2'}$ and $^5D_{1'} \rightarrow {}^7F_{1'}$ transitions.[62,65] The higher-energy side of the band (peaks at 14 520 and 14 410 $cm^{-1}$) correspond to emissions from the $^5D_{1'}$ level, while the lower-energy side mainly consists of contributions from the $^5L_{6'} \rightarrow {}^7F_{2'}$ transitions.

Although the bands at 18 850 and 18 440 $cm^{-1}$ cannot be assigned to either purely electronic or vibronic transitions, the energy difference between these bands and the lowest $^5L_{6'} \rightarrow {}^7F_{0'}$ transition (19 200 $cm^{-1}$) is suggestive of the presence of coupling between the electronic transition and $\nu_{IO}$ vibrational modes. These energy differences of ~350 and 760 $cm^{-1}$ are consistent with coupling involving both stretching and bending modes of iodate. In addition, the band centered at 16 490 $cm^{-1}$ is broader than expected for the $^5L_{6'} \rightarrow {}^7F_{1'}$ transition of $Am^{3+}$. Several scenarios are possible that could account for this observation. First, shoulders located on either side of the 16 490 $cm^{-1}$ peak, at 16 750 and 16 280 $cm^{-1}$, are shifted ~330 and 800 $cm^{-1}$ from the $^5D_{1'} \rightarrow {}^7F_{0'}$ electronic transition (17 080 $cm^{-1}$). These shoulders could possibly represent vibronic coupling between the $^5D_{1'} \rightarrow {}^7F_{0'}$ electronic transition and iodate vibrational modes. We have considered a second possibility that could contribute to the broad band at 16 490 $cm^{-1}$. The 16 490 $cm^{-1}$ band is shifted ~3000 $cm^{-1}$ from the excitation frequency (19 436 $cm^{-1}$) and could contain contributions from O−H Raman scattering, either as $H_2O$ or $HIO_3$. Although these contributions are not expected based on the X-ray structure, Raman experiments on the isostructural $Nd(IO_3)_3$ were performed. These experiments did not reveal the presence of any peaks consistent with O−H Raman scattering. Therefore, we have no basis to speculate the existence of $H_2O$ or $HIO_3$ in $Am(IO_3)_3$. Addtionally, the $Nd(IO_3)_3$ Raman spectrum lacked Stokes shifts in the 585 and 1035 $cm^{-1}$ regions, lending evidence to the possibility of vibronic coupling between the $^5L_{6'} \rightarrow {}^7F_{0'}$ electronic transition and iodate vibrational modes in $Am(IO_3)_3$.

The $^5D_{1'} \rightarrow {}^7F_{2'}$ transition, which was expected at ~12 000 $cm^{-1}$, is absent in the $Am(IO_3)_3$ profile under the conditions used to collect the other transitions. The absence of this band is surprising, since in a number of americium compounds[70−72] it has been reported as the second most intense band. The $^5D_{1'} \rightarrow {}^7F_{2'}$ transition is a magnetic dipole allowed transition and should be strong in systems where $Am^{3+}$ is located on a center of inversion.[73] However, its absence cannot be explained entirely by symmetry considerations alone. This is especially true for actinide systems since comparable strength between spin−orbit and electron−electron interactions limit the value of the Rusell−Saunders coupling scheme and strict adherence of the selection rules are unlikely. The phenomenon appears indicative of a process that quenches the emission selectively. A likely mechanism that can quench the $^5D_{1'} \rightarrow {}^7F_{2'}$ transition selectively is cross relaxation between neighboring cations. However, we have no direct evidence to discern among the various possibilities.

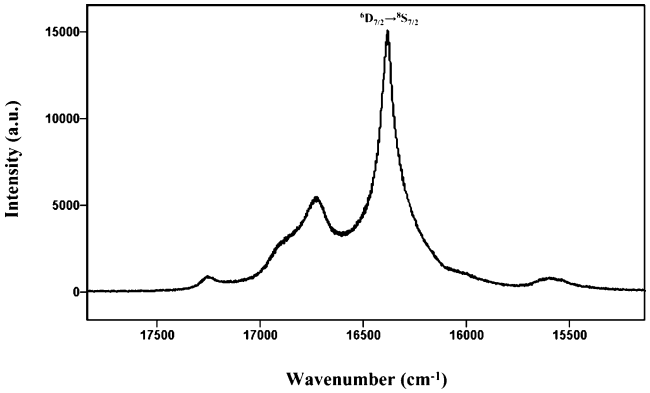


**Figure 6.** Emission spectrum of $Cm(IO_3)_3$ collected using the 457-nm line of an argon laser.

**$Cm(IO_3)_3$.** In addition to $Am(IO_3)_3$, we have also examined the photoluminescence properties of $Cm(IO_3)_3$. The emission spectrum from a single crystal of $Cm(IO_3)_3$, shown in Figure 6, has peaks at 17 250, 16 910, 16 750, 16 390, and 15 590 $cm^{-1}$, with a weak shoulder located at ~16 000 $cm^{-1}$. On the basis of the f-level structure of $Cm^{3+}$, the emission originates from the first excited $J = {}^7/_2$ state. The ground state, $^8S_{7/2}$, of the half-filled $5f^7$ configuration of $Cm^{3+}$ is spherically symmetric, and only a small splitting (few wavenumbers) of it is expected due to inner sphere coordinating ligands. As a consequence, the structured emission observed for $Cm(IO_3)_3$ is attributed to ligand field splitting of the emitting $J = {}^7/_2$ state. Ligand-field effects are expected to split this level into a maximum of four Stark components due to the low site symmetry of curium in the crystal structure.

The most intense emission band at 16 390 $cm^{-1}$ is assigned as originating from the lowest Stark level of the $J = {}^7/_2$ excited state, while the higher-energy splittings at 17 250, 16 910, and 16 750 $cm^{-1}$ are assigned to the remaining three Stark components. The observation of these four peaks is consistent with the low symmetry curium site ($C_1$) determined from the X-ray data.

Identifying the exact source of the low-energy bands at 16 000 and 15 590 $cm^{-1}$ is not straightforward, but they could arise from vibrational coupling with an electronic transition. Although the 5f electrons are considered to be localized and electrically shielded by the outer s an p electrons, bands resulting from the coupling of electronic and phonon excitations are routinely observed in the optical spectra of f elements,[74,75] especially so in actinide systems.[76] In $Cm^{3+}$-doped crystals of $YPO_4$ and $LuPO_4$, Liu et al. reported[77] that weak coupling involving P−O stretching and bending modes exist in these systems. In a curium $\beta$-diketonate complex, Nugent et al. have reported[78] that the emission profile consists

(70) Hubert, S.; Thouvenot, P.; Edelstein, N. *Phys. Rev.* **1993**, *B48*, 5751.
(71) Chudnovskaya, G. P.; Gavrish, Y. I.; Barbanel, Y. A. *Radiochimica* **1988**, *30*, 46.
(72) Chudnovskaya, G. P.; Dushin, R. B.; Kolin, V. V.; Barbanel, Y. A. *Radiochimica* **1985**, *27*, 545.
(73) Conway, J. G.; Judd, B. R. *J. Chem. Phys.* **1964**, *41*, 1526.
(74) Blasse, G.; Meijerink, A.; Donega, C. M. *J. Alloys Compd.* **1995**, *225*, 24.
(75) Blasse, G. *Int. Rev. Phys. Chem.* **1992**, *11*, 71.
(76) Hubert, S.; Thouvenot, P. *J. Lumin.* **1992**, *54*, 103.
(77) Liu, G. K.; Li, S. T.; Zhorin, V. V.; Loong, C.-K.; Abraham, M. M.; Boatner, L. A. *J. Chem. Phys.* **1998**, *109*, 1.

**Table 5.** Emission Energy for the $Cm^{3+}$ $^6D_{7/2} \rightarrow {}^8S_{7/2}$ Transition in Some Select Curium Compounds

| compound | energy ($cm^{-1}$) | ref |
|---|---|---|
| $Cm-SiO_3$[a] | 16 172 | 82 |
| $CmI_3$ | 16 213 | 79 |
| $Cm(IO_3)_3$ | 16 390 | this work |
| $CmBr_3$ | 16 604 | 79, 80 |
| $CmCl_3$ | 16 759 | 79, 81 |

[a] $Cm-SiO_3$ represents $Cm^{3+}$ in borosilicate glasses.

of weak components that are assignable to vibronic coupling with the electronic transition. Similar coupling could likely be the source of the 15 590 and 16 000 $cm^{-1}$ peaks in the emission spectrum of $Cm(IO_3)_3$ due to the following reasons. First, the intensity of these peaks is much lower relative to the most intense band at 16 390 $cm^{-1}$. Vibronic couplings usually provide very weak bands, as observed in Figure 6. Second, the energy difference between the lowest emitting level (at 16 390 $cm^{-1}$) and the two bands at 15 590 and 16 000 $cm^{-1}$ is ~800 and ~390 $cm^{-1}$, respectively. These energy differences roughly correspond to the energies of the $IO_3^-$ stretching and bending modes, respectively. Hence, it is logical to assume a coupling involving the transition from the lowest-energy crystal field component at 16 390 $cm^{-1}$ and the final vibrational quantum states of the $IO_3^-$ ligand. Unfortunately, we lack the ability to collect the emission spectra of radioactive samples at cryogenic temperatures, limiting our ability to glean more information on the coupling extent.

In Table 5, the emission energy of the $^6D_{7/2} \rightarrow {}^8S_{7/2}$ transition for $Cm(IO_3)_3$ is compared to that of selected solid-state curium compounds with well-characterized emission behaviors. The emission band red shifts on going from the trichloride to the tribromide and to the triiodide compounds[79−81] with the highest shift corresponding to borosilicate matrixes.[82] When compared to the chloride and bromide compounds, the emission band of $Cm(IO_3)_3$ is red shifted by about 2.2 and 1.3%, respectively. However, the emission band of the curium iodate is blue shifted relative to $CmI_3$.

For electronic transitions involving metal orbitals that directly participate in bonding, the relative decrease in interelectronic repulsion in going from the free ion to compounds is known to cause a red shift.[66,67] The relative decrease in percent of the interelectronic repulsion is evaluated from the red shifts and is correlated with the nephelauxetic effect.[66,67,82,83] However, unlike the transition metals, where d orbitals can participate directly in bonding, the cause for nephelauxetic effects in f-element spectroscopy is not well understood. Since the energies of f levels are primarily governed by spin−orbit coupling, it is not clear if the shift represents a weakening of the coupling.

Two possible mechanisms have been suggested by Jorgensen,[84] where covalent interactions with neighboring ligands were considered important: (a) some participation of the f orbitals in the formation of molecular orbitals; (b) transfer of some part of the ligand electron density to the unfilled s and p orbitals. Experimentally, the red shift in f−f transitions has been correlated with the basicity of the coordinating ligand; the largest shift is caused by the most basic ligand. According to Sinha's lanthanide nephelauxetic effect derived from spectroscopic data, $O^{2-}$ is the most basic and $F^-$ the least basic ligand.[83] While the band shifts observed in 4f-lanthanide species are small, shifts as high as 1100 $cm^{-1}$ have been noted in actinide systems.[85,86] For the $^5L_6$ level of Am(III) a nephelauxetic shift of up to 5.6% has been noted within the halide series ($F^-$ to $I^-$ systems).[86] The data are consistent with previous results where an increased red shift has been correlated with a decreased electronegativity of the halide in the emission spectra of $CmX_3$ (X = F, Cl, Br, I).[85] Thus, based on the spectroscopic comparisons described here, it is inferred that the electron donating ability of the iodate ligand should be placed between that of $Br^-$ and $I^-$ ligands.

## Summary and Conclusions

This report deals with our continuing studies into the chemistry of the 4f and 5f iodates. Herein, we have expanded the Type I anhydrous family of iodates $M(IO_3)_3$ (M = Ce−Nd, Sm−Lu, Y, Cm) to include americium. By use of single-crystal X-ray diffraction, we have determined the structure of $Am(IO_3)_3$ and studied the effects of self-irradiation on it's structure with time. Raman spectroscopy has also been used to further characterize this material. We have assigned the symmetric and asymmetric modes of the iodate anions in $Am(IO_3)_3$ and have compared them with values reported for other lanthanide and actinide iodates. Photoluminescence data collected for both $Am(IO_3)_3$ and $Cm(IO_3)_3$ are also reported here for the first time. Electronic transitions for $Am^{3+}$ and $Cm^{3+}$ in $Am(IO_3)_3$ and $Cm(IO_3)_3$ have been assigned based on these measurements. The spectra of both materials appear to be consistent with the presence of vibronic coupling between electronic transitions and $IO_3^-$ vibrational modes.

Finally, we have studied the effects of self-irradiation in $Am(IO_3)_3$ and compared them to those observed for $Cm(IO_3)_3$. Although overall cell expansions with time are found for both $Am(IO_3)_3$ and $Cm(IO_3)_3$, a different mechanism of expansion appears to be operational. The structural changes are attributed mainly to alpha decay and recoiling nuclei in the $Am(IO_3)_3$ as compared to neutron irradiation and fission fragments arising from spontaneous fission in $Cm(IO_3)_3$.

**Acknowledgment.** Support for this work was provided by the Division of Chemical Sciences, Geosciences and

(78) Nugent, L. J. J.; Burnett, L.; Baybarz, R. D.; Werner, G. K.; Tanner, S. P.; Tarrant, J. R.; Keller, O. L. *J. Phys. Chem.* **1968**, *73*, 1540.
(79) Stump, N. A.; Murray, G. M.; Del-Cul, G. D.; Haire, R. G.; Peterson, J. R. *Radiochim. Acta* **1993**, *61*, 129.
(80) Murray, G. M.; Del Cul, G. D.; Begun, G. M.; Haire, R. G.; Young, J. P.; Peterson, J. R. *Chem. Phys. Lett.* **1990**, *168*, 473.
(81) Barbanel, Y. A.; Chudnovskaya, G. P.; Gavrish, Y. I.; Dushin, R. B.; Kolin, V. V.; Kotlin, V. P. *Radioanal. Nucl. Chem.* **1990**, *143*, 113.
(82) Assefa, Z.; Haire, R. G.; Stump, N. A. *Mater. Res. Soc. Symp. Proc.* **1999**, *556*, 359.
(83) Sinha, S. P. *Complexes of the Rare Earths*; Pergamon Press: Oxford, 1966; p 106.
(84) Ryan, J. L.; Jorgensen, C. K. *J. Phys. Chem.* **1966**, *70*, 2845.
(85) Barbanel, Y. A.; Klokman, V. R.; Kotlin, V. P.; Kolin, V. V.; Gavrish, Y. I.; Smirnov, A. N. *Radiokhimiya* **1982**, *24*, 580.
(86) Barbanel, Y. A. *Radiochemistry* **1996**, *38*, 27.

Biosciences, OBES, USDOE, under Contract DE-AC05-00OR22725 with Oak Ridge National Laboratory, managed by UT-Battelle, LLC and by the U.S. Department of Energy through Grant DE-FG02-01ER15187 (to T.E.A.-S). The Am and Cm isotopes used in these studies were supplied by the USDOE through its production program at ORNL. Dr. Radu Custelcean and Dr. Bruce Moyer are thanked for their generous allocation of X-ray diffractometer time. This research was supported in part by an appointment to the Oak Ridge National Laboratory Postdoctoral Research Associates Program (to R.E.S.) administered jointly by the Oak Ridge Institute for Science and Education and Oak Ridge National Laboratory. We are grateful for the valuable suggestions from anonymous reviewers.

**Supporting Information Available:** The X-ray crystallographic file in CIF format is available for $Am(IO_3)_3$. This material is available free of charge via the Internet at http://pubs.acs.org.

IC050386K